International Journal of Engineering Trends and Technology
ISSN: 2231-5381/ https://doi.org/10.14445/22315381/IJETT-V74I3P119

Volume 74 Issue 3, 258-271, March 2026

Original Article

Blockchain-Based Federated Learning Framework for Melanoma Detection and Classification

M. Kalaivani[1], SK.Piramu Preethika[2]

[1,2]*Department of Computer Science, Vels Institute of Science Technology & Advanced Studies, Chennai, India.*

[2]*Corresponding Author : preethikamanikandan@gmail.com*

Received: 26 May 2025 Revised: 29 January 2026 Accepted: 06 February 2026 Published: 28 March 2026

Abstract *- Melanoma is a deadly cancer; the patient's survival outcomes are based on the early detection and accuracy of the prediction. The data sharing of patient medical information in centralised systems poses privacy risks and regulatory challenges. To encounter this issue, the Secured Federated Learning framework is designed for melanoma detection and classification that ensures data security, integrity, and privacy in a decentralized manner using Blockchain Technology. The local image processing techniques leverage the HAM10000 dataset that comprises 10000 skin lesions of seven types of skin cancer, incorporating the U-Net-based image segmentation, CapsNet-based feature extraction, and VGG16, VGG19, and Inception V3 as pretrained models in the Ensemble transfer learning for classification of melanoma types. The global model shares the Deep learning based training model and datasets with the local model, allowing multiple healthcare institutions to work collaboratively. The smart contracts ensure trust, immutability, and secure aggregation in the block model updates. The proposed framework outperforms the conventional one by 93% accuracy and test error reduction to 0.01% for 100 iterations. Thus, the proposed work highlights a secure decentralised system for melanoma diagnosis using advanced image processing techniques.*

Keywords *- Melanoma, Skin Cancer, CapsNet, Ensemble Transfer Learning, Federated Learning, Blockchain.*

1. Introduction

Melanoma skin cancer has a high percentage of death rate, found in the cells that cause melanin production, called melanocytes. The genetic mutations, Ultraviolet Rays (UV), skin inflammation, and abnormal melanin cells contribute to the occurrence of melanoma. Melanoma needs early prediction to save lives. Geographical disparities play a major role in melanoma, with fairer-skinned people and high-sun-exposed areas, such as North America, Europe, New Zealand, and Australia, being recorded [1]. According to the American Cancer Society, the occurrence of melanoma among white people is 3% of the 33 population, among black people is 0.1% of 1000 population, and among Hispanic people is 0.5% of 200 population. Usually, the melanoma kind of skin cancer is detected by visual clinical examination, dermoscopy, skin biopsy, and laboratory tests. Based on the ABCDE rule, the Dermatologist detects melanoma by examining the skin lesions that are unusual. The ABCDE rule is based on parameters like Asymmetry, Border, colour, Diameter, and evolution of the skin lesion. The survival rate of melanoma is increased by early detection and advances in medical treatment. The American Cancer Society produces statistics of the survival rate of melanoma, showing 5-year survival rates using the SEER (Surveillance, Epidemiology, and End Results) database by grouping the cancer based on the spread of skin, like localised, regional, and distant, which helps to determine the stages, like I, II, III, IV, and V of melanoma. The key aspect in raising the survival rate of melanoma is based on early prediction and diagnosis. The growing rate of melanoma requires a larger number of dermatologists for early prediction, which is quite challenging. The intervention of Machine Learning (ML) and Deep Learning (DL) algorithms helps in the early prediction of melanoma by training the system with melanoma image datasets. These systems efficiently determine the melanoma, its stages, and its types. The melanoma patients require a decentralised communication network to approach the medical advisory that can be provided using federated learning, which maintains the integrity of the patient data by training the patient data on servers. Blockchain technology, by integrating AI (Artificial Intelligence) with the cybersecurity systems, helps in maintaining the data security of patient data.

The melanoma patient survival rate can be increased by early detection of cancer, which remains challenging due to variability in skin lesion features. Most of the image processing techniques fail to observe the morphological features in the skin lesion images to identify their type. The feature extraction of skin lesion images requires capturing the spatial relationships for efficient prediction of melanoma. The machine learning techniques employed fail to maintain the integrity and security of the patient information in the

healthcare domain. Therefore, the existing literatures lack an integrated framework of a privacy-ensured decentralised system with efficient training models that can extract the spatial-based higher-order features for improving the accuracy of melanoma detection along with the early diagnosis. Therefore, the multi-hospital environment has to access the information of patients without the need for the raw information, which is possible using Federated learning with authentication, which is provided by the Blockchain systems. This research contributes to the early prediction and determination of types of melanoma using the morphological features, using the CapsNet (Capsule Network) for feature extraction, ensemble learning for classification, and Long Short Term Memory for real-time basis in the local model of the Federated learning framework using the Blockchain technology for securing the patient data sharing and processing. The training model efficiently obtains the gradients with high-level spatial features using the generalised ensemble learning method, using real-time processing that helps the Dermatologist in the early detection without the need for actual raw data of the patient. The paper is organised as follows: i) Introduction, ii) Related works, iii) Melanoma Feature Extraction and classification, iv) Blockchain-based Federated Learning framework, v) Results and discussion, and vi) Conclusion.

2. Related Works

2.1. Clinical Survey

The melanoma, based on its clinical, morphological, and histopathological [3] characteristics, is divided into many kinds: Superficial Spreading Melanoma (SSM), Nodular Melanoma (NM), Lentigo Maligna Melanoma (LMM), Acral Lentiginous Melanoma (ALM), Desmoplastic Melanoma (DM), Mucosal Melanoma, and Ocular Melanoma. The types of melanoma vary by age, sex, location of occurrence, appearance, growth phase, pattern-wise, thickness, etc, where some of the important features are listed in Table 1.

Table 1. Clinical features survey

Type	Stat	Age	Color	Features	Growth Pattern	Growth Phase	Location
SSM (Superficial Spreading Melanoma)	70%	30-50	Multiple colors	Flat or raised lesion, irregular border	Slow growing	Horizontal	Trunk (men), Legs (women)
NM (Nodular Melanoma)	10-15%	50-60	Black, blue, brown, pink	Dome-shaped, non-ulcerated or ulcerated and bleeding	Rapid growth	Vertical	Head, neck, trunk
LMM (Lentigo Maligna Melanoma)	5-10%	>60	Tan-brown	Flat, slow-darkening, varying nodular	Slow growing	Radial	Face, neck, hands
ALM (Acral Lentiginous Melanoma)	<5%	>40	Dark brown or black	Aggressive, nail discoloration, irregular patch	Slow growing	Aggressive	Palms, soles, under nails
DM (Desmoplastic Melanoma)	<4%	>60	Skin-coloured	Complex, scar-like lesion, high recurrence risk	Local invasive	Deep tissue invasion	Head, neck, trunk
Mucosal	1%	>50	Pigmented / non-pigmented	Very rare, darker skin tone	Aggressive	Late detection	Mouth, nose, esophagus, genitals, anus
Ocular	3-5%	50-70	Dark spot in the eye	Rare, blurry vision, floaters	Slow/aggressive	Metastasize	Eye

The variations in the melanocytes are due to cytomorphological features and exhibit favorable terms of S100 proteins, Melan-A, and HMB-45 (Human Melanoma Black) [4]. Based on the stromal changes in the melanocytes, the cell mutations take place that result in malignant melanoma. Cutaneous melanoma [5] is mainly caused by UV radiation exposure in the face, hands, and legs, and has an occurrence rate of 90% among the various melanomas. Cluster-based morphological analysis is done in [6], where the different kinds are based on typical, nevus-like, amelanotic-based, keratosis, and lentigo-based. The metastatic melanoma [7] is a kind that spreads the cancer cells to the distant organs of the human being, where it can be diagnosed at the cellular level and based on the number. Using the histologic features [8], the melanoma in 336 patients was studied using histology, HMB45, S-100, Vimentin (VIM), Cytokeratin (CK), and FM (Fontana Masson). There are several unusual characteristics of malignant melanoma [9] that lead to various kinds of it that

can be diagnosed with genetic tests, along with the histologic feature analysis, which helps in the early detection of melanoma. Instead of morphological features, genetic characteristics are taken as a parameter to identify the melanoma using the BRAF and NRAS gene mutation, as carried out in [10], where it is identified that the BRAF genetic mutation shows good variance in the malignant cells. The molecular analysis [11] for melanoma detection and classification is done using Clark's model employing the BRAF, NRAS, and GNAQ gene mutation levels.

2.2. Computer Vision Approach

The melanoma image datasets are feature extracted, segmented, classified, and predicted accurately using various datasets like ISBI challenge 2016, DERMIS and DERMISQST, Mednode dataset, ISIC archive, 2018 ISIC challenge, PH2 dataset, Dermofit Image library, 2019 ISIC challenge, Dermnet, and Interactive dermoscopy atlas using Deep Neural Networks (DNN) like Transfer learning, Convolutional Neural Network, ensemble, and hybrid are reviewed in [12]. The ensemble machine learning technique for three different feature sets, based on the borderline of the segment and dimensionality-reduced image using the PCA analysis, is carried out in [13], showing an accuracy of 95.2% for an ensemble of two RF, SVM, BoF, and kNN algorithms.

The benign and malignant melanoma are classified using the RESNET [14] based CNN model, using 4 variants, based on transfer learning using the ISBI 2017 challenge datasets, showing 87% accuracy. However, it does not seek the prognosis of the disease. In [15], deep learning models like CNN, CapsNet (Capsule Network), and Ensemble learning are used to classify skin lesions using the Vision Transformer, with the help of image embeddings, which provided good feature extraction. The three kinds of datasets, ISBI 207, ISIC 2017, and PH2 datasets, are used for melanoma detection with an encoder and decoder by a multi-scale and multi-stage approach and a lesion classifier using the neural network of deep layers in [16]. The conventional CNN model is used in [17] to provide a computer vision approach to melanoma detection with an accuracy of 81%.

The Capsule Network [18] is used in melanoma detection based on the spatial relationship and dynamic hierarchical routing that extracts the features of the skin lesion for better classification. The capsule vectors [19] with the learnable bias in a controlled manner were used to classify the skin lesions for the detection of benign and malignant melanoma, showing 95.2% accuracy using the spatial relationship between capsule layers. Instead of a 9×9 kernel size, the capsules used a 31×31 kernel size in [20] to overcome the underfitting problem, where the FixCaps produced 96.45% efficiency with the large kernel size. The privacy preservation of skin disease patient data is carried out using the federated learning approach [21] for 500, 1000, and 2000 users using the CNN kind of classification of skin lesions. The federated learning model is applied to Breast Cancer Detection [22] using a DCNN model, which maintains the integrity of the patient data at the local model and global server model, and produces a good efficiency of 91% with a homomorphic encryption model. The translation of image processing from CNN to Capsnet architecture is well explained in [23] using the medical image segmentation, where the capsule layer function, dynamic routing, and softmax function using medical image data analysis are presented.

By fusing the low-frequency and high-frequency components of the image, the different dimensions are detected automatically using the Automated Octave CapsNet [24] in the medical image classification of seven different disease datasets. In the CapsNet architecture, the computational complexity is high compared to the CNN architecture, as it undergoes the spatial relationship finding and dynamic routing processes.

The computational complexity increases the time consumption, which is reduced in [25] using the new method called Time Efficiency- CapsNet, where the number of layers is decreased in processing the medical image dataset, and showed an 11% reduction in complexity. The CapsNet is the successor of the CNN model, where the instantiation parameters, hierarchical dynamic routing, spatial relationship between features, and capsules work on different functions of the images are provided in [26] as a survey, and it is applied in the MNIST dataset to show its performance.

The Federated application using blockchain technology in local and global server-based based, on the security issues arising in almost all fields, is discussed in [27], where the bottleneck issues in the central server to maintain data privacy are addressed. Biscotti [28], the blockchain-based federated learning approach, multi-party security by employing the distributed ledgers based on workloads to overcome the centralised server trust issues in the federated learning approach. The prospective study is carried out in [29] for melanoma classification using the federated learning and transfer learning approaches for melanoma datasets based on public and private availability are reviewed.

In the existing literature, the melanoma occurrence due to sun exposure affects the epidermis by gene mutation of BRAF and NRAS of melanin, which requires early detection to reduce the death of the patient. Deep learning models using CNN highly influence the accurate predictions but lack the extraction of high-level features that help in analyzing the ABCDE parameters. In the existing models, security and privacy become more concerns; therefore, the proposed work chose the Blockchain-based Federated Learning framework utilising the high capsule-based CapsNet-based Ensemble learning system to produce a high level of prediction accuracy with a privacy-preserved system.

3. Melanoma Feature Extraction and Classification

Melanoma is the deadliest among the skin cancer types; the survival of the patient can be improved with early prediction of occurrence. Early prediction is possible through various clinical tests analysed by the Dermatologist. With the intervention of a computer vision approach, the early prediction of melanoma is possible using the lesion images taken from the patient. From the survey, various methods are employed in the prediction of melanoma detection and classification.

It is seen that the Convolutional Neural Network is the pioneer in feature extraction, which has shown high accuracy in image processing techniques. However, the CNN architecture deals with the lower-level features of the image that have less spatial relationship with the previous layers. The pooling layer in CNN actually reduces the important information. The CapsNet architecture is the inheritor of the CNN architecture, using different capsules for finding the spatial relationship and dynamic routing purposes without the pooling layer in CNN. This helps to obtain the characteristics of the image from low feature level to high feature level, which helps significantly in the classification processes.

The ABCDE rule [30] in melanoma detection is constructive, where the complete form is listed below,

- A- Asymmetrical pigmentation
- B- Borders are irregular for malignant melanoma
- IIIC- Colour of the lesion is not uniform
- D- Diammeter more than 6mm is an unusual size that is taken for melanoma detection. E- Evolution of cancer cells varies the size, colour, and shape of the melanoma-affected area.

The above-listed ABCDE rule is used for melanoma detection based on the growth phase and pattern. The stages of melanoma are detected and treated accordingly. In this work, along with the melanoma detection, the classification of different types of it is done. The different types of melanoma and their morphological features are listed in Table 2. Superficial Spreading Melanoma (SSM) [31] is an irregular edge spotted on the skin due to outgrowth of melanocytes on the skin, where the rate is less compared to other kinds.

Nodular Melanoma (NM) [32] is the fastest-growing melanoma of blister kind on the skin, characterized by its structure. Lentigo Maligna Melanoma (LMM) [33] is a type of melanoma that belongs to a rare cases that occur in the head and neck with a slower growth rate mainly due to sun exposure. Acral Lentiginous Melanoma (ALM) [34], where it starts in dark colour and spreads more easily with a blurred and irregular border. Desmoplastic Melanoma (DM) [35] is a scar that looks like a spot and tends to develop on the sun-exposed areas of the skin.

Table 2. Features of different types of melanoma

Type/ Parameter	SSM	NM	LMM	ALM	DM
Asymmetry	1.3-1.8	1.5-2	1.2-1.5	1.4-1.9	1.3-1.7
Border irregularity	Jagged	Slight irregular	Fuzzy	Diffuse	High irregular
Diameter	6-20mm	5-15mm	8-30mm	7-20mm	10-40mm
Irregular streaks	80%	60%	40%	50%	42%
Atypical pigment network	70-80%	30-50%	50-60%	40-55%	25-45%
Dotted vessels	55-70%	60-80%	35-50%	40-55%	25-45%
Surface elevation	1-4mm	2-6mm	1-3mm	1-5mm	2-7mm
Blotch	70-85%	75-90%	60-75%	50-65%	40-60%
Ulceration	30-50%	50-70%	10-30%	20-40%	15-35%

Table 3. feature extraction formulation

FEATURES	FORMULATION
Texture Features	Contrast= $\sum_{i,j} p(i,j)(i-j)^2$ Homogeneity=$\sum_{i,j} \frac{p(i,j)}{1+\|i-j\|}$ Entropy=-$\sum_{i,j} p(i,j) * \log(p(i,j))$
Edge And Border Irregularity Features	Fractal dimension=$\frac{\log N}{\log(1\backslash\epsilon)}$ Perimeter irregularity=$\frac{Perimeter}{4\pi * Area}$ Circularity=$\frac{4\pi \times Area}{Perimeter^2}$
Colour Variation Features	$\mu_C = \frac{1}{N}\sum_{I=1}^{N} I_C(i)$ $\sigma_c = \sqrt{\frac{1}{N}\sum_{i=1}^{N}(I_c(i)-\mu_c)^2}$

	Color spread=$\frac{\max(I)-\min(I)}{\max(I)}$
Shape And Asymmetry Features	$AI = \frac{\lvert A_L - A_R \rvert}{\max(A_L, A_R)}$ $E = \sqrt{1 - \frac{b^2}{a^2}}$
Capsule Feature Representation	$v_j = \frac{\lVert s_j \rVert^2}{1+\lVert s_j \rVert^2} \frac{s_j}{\lVert s_j \rVert}$ $c_{ij} = \frac{exp(b_{ij})}{\sum_k exp(b_{ik})}$ $s_j = \sum_i c_{ij}.u_i$
Parameters used : p(i,j)= probability of pixel pairs N- Number of self-similar structures, ϵ- scale factor μ_c- mean color intensity, σ_c-S. D , $I_c(i)$= Pixel intensity A_L &A_R – Areas of the left and right halves of the lesion a-Major axis length, b-minor axis length s_j- summed input to capsule j, v_j=squashed output $u_{i=}$ low layer capsule outputs, $c_{i,j}$- coupling coefficient	

Figure 1 shows the proposed work of using the CapsNet architecture for feature extraction and Ensemble transfer learning for melanoma classification processes. In the first step, the image dataset undergoes resizing, normalising the image scale, and data augmentation. The image segmentation is carried out using the CNN model, where the area in the lesion where the affected part is taken for processing. This helps in concentrating on the affected areas rather than the standard parts in the images. Primarily, the U-Net-based architecture is used for image segmentation due to up-sampling, which produces high resolution and perfectly obtains the boundaries for the diseased part in the medical images.

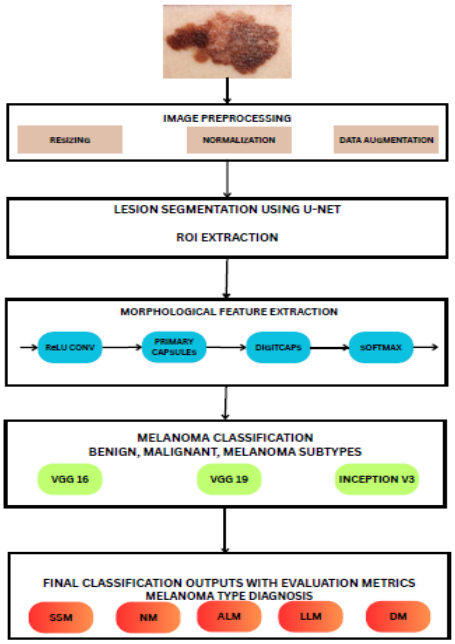

Fig. 1 Proposed work

Morphological features are the main characteristics used for feature extraction from the segmented skin lesion. Using the morphological characteristics based on asymmetry, border, diameter, irregular streaks, and dotted vessels, the features are obtained from the primary capsules based on the spatial relationship. The digitcaps augment the primary capsule output, and the softmax operation occurs within the CapsNet architecture. The features from the CapsNet architecture are pretrained in the transfer learning model using VGG16, VGG19, and Inception V3. These three are used to provide an accuracy of 92% to 93% which is of a deep CNN type. Inception V3 is the fastest of the three methods. The pre-trained model helps extract higher-level features based on

symmetry, colour, area, borders, irregularity, and shape. The output from this model helps in training the model for future processes. The feature vectors from the CapsNet model are used to find the characteristics listed in Table 3 to obtain the patterns for the classification process. The output of the model is fed into the ensemble learning of a pretrained model, where the melanoma classification based on its types is detected. The types are obtained by the classification pattern of morphological features extracted from the segmented lesion. The classification is assessed by the evaluation metrics, where the final output predicts whether the skin lesion is benign or malignant and its types.

4. Secured Federated Learning Framework Using

Federated Averaging, a Federated learning model [36], is the decentralized mode of data transfer between the local and global models. The local models are present with the clients, where the information from the clients is recorded. The global model defines the training model and distributes it to the local model for communication. The main advantage of the federated learning approach is that the local model can maintain the integrity of the client's data by only upgrading the weights or gradients to the global model. In our proposed work, the FedAvg framework is adopted to maintain the communication between the patient and hospital nodes. The global model fixes the training model of melanoma detection and classification using the CapsNet and Ensemble Transfer learning, and distributes the information to the local model for the patients. The patients using the skin lesion images collected using either medical equipments or smartphones train the lesion image in the local model and update the weights to the global model. The global model aggregates the weights and updates the hospital node. This proposed approach helps in the early detection of melanoma, and if the melanoma is detected, it helps to classify the type of melanoma using the proposed image processing method.

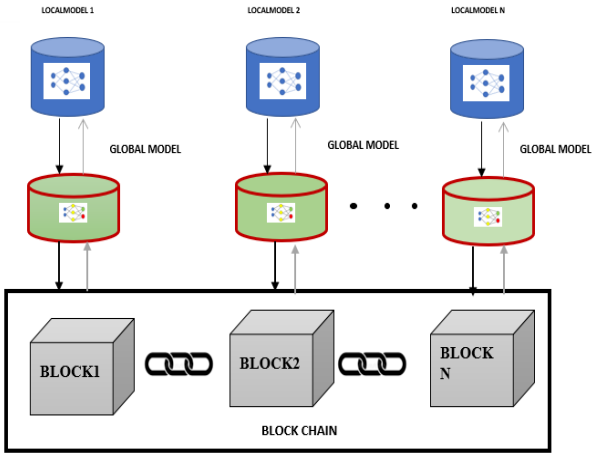

Fig. 2 Blockchain-based federated learning framework

From a security perspective of the patient data, the Federated learning approach is more prone to poison attacks [37]. The local model data are poisoned by the malicious clients, which leads to the misleading classification of patient data in the global model. It also degrades the performance of the local and global models. In federated learning, the local model only transfers the gradients to the global model. The global model does not verify whether the weight updates are from an authenticated patient. This leads to a security issue of falsified gradients, which leads to the misprediction of patients' disease. In the Federated learning approach, Blockchain technology is included to improve the security of the patient's data, as shown in Figure 2. The Blockchain adds trust to the patient's data by clients' registration on the Blockchain, smart contracts that validate the global model updates, and storage of past updates that are auditable. The patient signs their local model gradients using the digital signatures, and smart contracts are used in the global model to test and maintain a history record. The Blockchain actually fixed the global model and gets the aggregated information about the local models of various patients. In the Blockchain to ensure the authenticity of local clients, the Euclidean distance is computed to the local models based on Krum, and the updates present within the threshold (majorities) are chosen.

This helps reduce suspicious anomalies in the local models. Figure 3 shows the flow of information in the local model, global model, and Blockchain. The Blockchain registers the clients and distributes the training model to the global model. The training model and datasets used by the local clients are shared with the global model. The local client performs image preprocessing, local training, and feature extraction using the CapsNet and Ensemble transfer learning model for melanoma classification. Long Short Term Memory is used for sequential data aggregration og past and previous weights from the local clients and updates the global model. The global model aggregates the weights from the local clients and stores them in the corresponding client blocks, and assigns a hash function, client ID, time stamp, weights, and rounds value. This blockchain-based Federated learning framework will run for particular rounds and a time duration. After that, the new global model is initiated and fixes the local clients based on it.

The client-side algorithm at the local model is described for melanoma classification using the decentralized FL system. The local model receives the update from the global model and obtains the dermoscopic image from the patient. Based on the global model update, the image processing of dermoscopy is done using U-Net-based image segmentation, feature extraction using the CapsNet architecture, and ensemble transfer learning is used for classification. The local model updating to global is done using the weighted average. LSTM is used to predict and update the global model using the past and present estimated values.

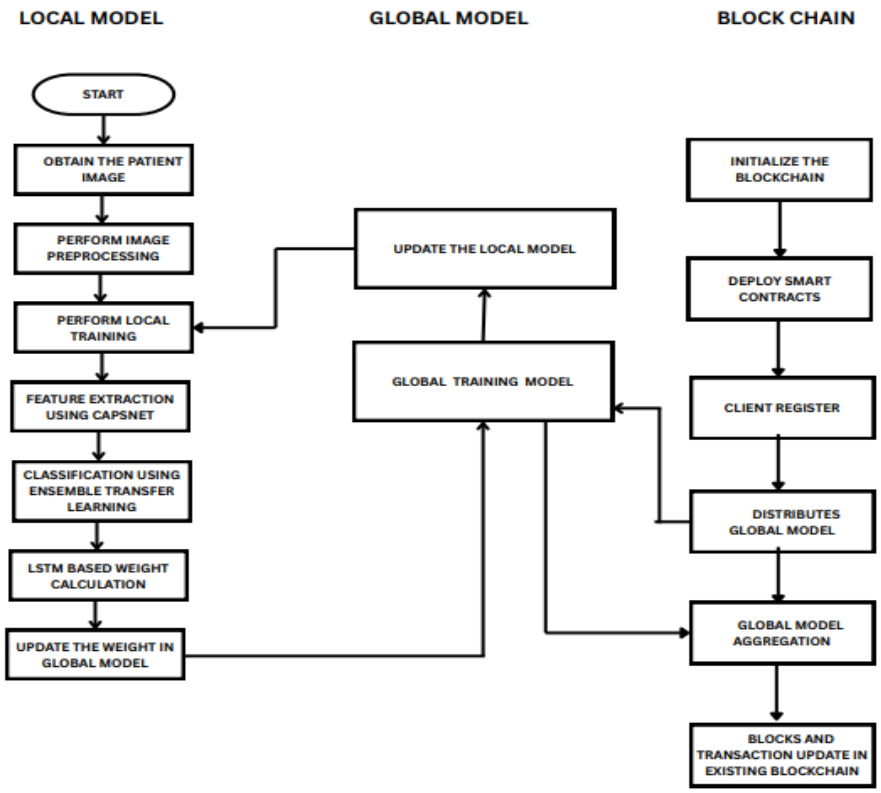

Fig. 3 Flow chart of the Proposed Framework

ALGORITHM: LOCAL MODEL (CLIENT-SIDE)

INPUT: Local Image Dataset, D
INPUT: Update from Global Model

1. Load dermoscopic lesion images, Ii
2. Lesion segmentation using a U-Net-based CNN for the lesion region
   Segi=CNN-U-NET(Ii)
3. Feature extraction using CapsNet using a Segmented lesion for spatial features.
   Fi=CapsNet(Segi)
4. Ensemble Transfer Learning based classification of feature-extracted image
   C1i=VGG16(Fi)
   C2i=VGG19(Fi)
   C3i=InceptionV3(Fi)
5. Prediction using weighted Average
   Finali=weightedavg(C1i, C2i, C3i)
6. LSTM-based prediction update using past and present predictions
7. Updatei=LSTM(Pasti, Presenti)
8. Fine-tune LSTM on updated prediction, Fi
9. Compute Local Weight Update
10. Θi=localtrain(Fi, updatei)
11. Upload Θi to Global Model

The blockchain integration of the federated learning algorithm is provided in the global model in the server-side operation. In the first step, the global model updates the local clients and obtains the smart contracts for the local clients from the Blockchain. The updates from the local model are verified via the smart contracts based on the similarity threshold value for acceptance. The accepted models alone were aggregated using the weighted federated averaging approach. To ensure the security of data, the updates from the global model are stored in the blockchain ledger for further processing.

ALGORITHM: GLOBAL MODEL

1. Broadcast θ to all the local clients by the Global model
2. Obtain smart contracts for all the clients from the Blockchain
3. Local model weight updates, θ1, θ2, …, θN
4. Verify via smart contract
5. for i=1:N
6. If $\|\theta_i - \theta_{i-1}\| < threshold$, $\|\theta_i - \theta_{i-1}\| < threshold$
7. Accept θi
8. else
9. Reject θi
10. end if
11. end for
12. Aggregation using the Federated Avg model
13. Favg= $\sum(|D_i|/\sum D_N) * \theta_i$, $\sum(|D_i|/\sum D_N) * \theta_i$
14. Store Favg in the Block blockchain ledger.

The blockchain framework for federated learning for the melanoma classification algorithm is provided. The smart contracts information for the client and the initialisation of the global model are done. Based on the smart contracts provided by the clients, the ledger stores the updates from the global model for every local client. Ledger updates are performed using the global model for the local models. The aggregated weights are stored in the ledger. Based on the convergence, the training rounds are carried out.

ALGORITHM: BLOCKCHAIN FEDERATED LEARNING FRAMEWORK

1. Initialise the smart contract for local clients
2. Initialise the Global Model
3. for i=1:t
4. for j=1: N
5. Receive θ_t, θ_t from the global model
6. Train local models
7. Upload θ_i, θ_i to the global model
8. Upload Favg to Blockchain
9. Verify updates by smart contracts
10. Aggregate Favg
11. Update the ledger from the global model for local clients
12. Distribute θ_{t+1} , θ_{t+1} to clients
13. if $\|\theta_{t+1} - \theta_t\|$, $\|\theta_{t+1} - \theta_t\|$ <max(t)
14. Break;
15. else
16. Continue;
17. end if
18. end for N
19. end for t
20. Update the Global model

5. Results and Discussions

5.1. HAM 10000 DATASET

For the proposed work of melanoma detection and classification, the HAM10000 dataset [38] is used, which contains collectively 10000 training pigmented skin lesion images of seven skin cancer types. This dataset contains more than 1000 melanoma-based skin lesions that help in the training and validation of the proposed work. It provides clinical-grade dermoscopic skin lesions taken using varied lighting, population, sex, age, and skin types. The source of the datasets is formed from Australia and the ViDIR group, Vienna, Austria. The image format is 600×450 pixels. The dataset contains image directory files, image metadata, image filename, label, hispathology/consensus-based diagnosis confirmation, age of the patient, patient sex, localisation of the skin image, and lesion ID. It is publicly available [39], curated, and cleaned images.

5.2. Image Processing

5.2.1. PreProcessing

The image preprocessing of the HAM10000 dataset is done primarily, where the image size of 224×224×3 and 229×229×3 (for inception) is obtained in the RGB colour space. The pixel values are rescaled to [0,1] using the function img/255. The normalised images undergo DullRazor via OpenCV for hair removal to obtain morphological operations. Gaussian blur is used for noise removal of the function cv-GaussianBlur (image, (5,5), 0). The contrast enhancement was done using the CLAHE using the Lab colour space. Images are then rotated, 0.2 width shifted, 0.2 height shifted, 0.2 zoomed, and horizontally flipped.

In the image segmentation, U-Net is used; the images after preprocessing are taken as input of size 224×224×3. It takes four down-sampling blocks, which have 64, 128, 256, and 512 filters to perform the base block function, and the last down-sampling block is the last. This provides the double convolution operation in the successive layers of the U-Net sample blocks based on the depth. The bottleneck layer of 1024 filters is where the decoding processes are done by transposed convolution, concatenation, and conv2d (ReLu) functions. The output activation is done using the Sigmoid function for the binary mask. The loss function is calculated using the Dice loss and cross-entropy. The Epochs of 25 using the Adam optimiser with a learning rate of 1e-4. The output is the binary lesion mask shown in Table 5.

5.2.2. Feature Extraction

The CapsNet architecture is used for feature extraction based on its various parameters listed in Table 3, which are calculated to obtain the type of melanoma present in the lesion image. The kernel filter size of 9 is used to perform the ReLU function to obtain the low-level features of the images.

After that, the primary capsule layer of size 8 is taken to obtain the high-level features of values like edges, orientation, texture, and angle. The output from complete 32×32×256×8 is converted to 10 capsules in the Digitcaps, where the convergence of features from the parent node of low features to the child node of high feature levels is done. The Softmax function is used to normalise the output of digitcaps, and the reconstruction loss is calculated to obtain the system performance. The parameters used for the CapsNet architecture are provided in Table 4.

Table 4. CapsNet feature extraction parameters

PARAMETER	VALUES
Input shape	224×224×3(VGG)
Number of filters	256
Kernel Size	9
Primary Capsules	32channels of 8D capsules
Digitcaps	16D capsule vectors
Routing Iterations	3
Loss function	Margin loss
Reconstruction	3-layer FCC
Optimizer	Adam
Learning rate	0.001

5.2.3. Ensemble Learning

The features extracted from CapsNet and the values like asymmetry, border irregularity, diameter, percentage of dotted vessels, and percentage of irregular streaks are calculated and mentioned in Table 5. The transfer learning process is done using the image resize of 224×224×3 and by interpolation to 229×229×3 for Inception V3. The weights are based on ImageNet using a dense layer of 512, dropout 0.5, and 7 classes for the softmax function using the library GlobalAveragePooling2D. The average output across 3 classes is used as the output when using soft voting methods. The LSTM for fine-tuning updating of the weight gradient features is accessed by 256 input features per time step of 128 hidden layers and a dropout of 0.3.

5.3. Blockchain-Based FL Framework

The TensorFlow FLL is used for the framework design, and the Ethereum Simulator for the Blockchain Network. The Hyperledger Fabric SDK is used for smart contracts and client chain interactions. Flask APIs are used for off-chain model weight exchange. Python and Docker containerize the local clients. The Proof of Authority consensus-based algorithm is used in blockchain networks. The block time of 5 to 15 seconds is used for training the local models. In the smart contract, the client registration, model update verification, and reward system are carried out. The chain contains data like the Hash of model weights, timestamp, round ID, and client ID. The secure cloud is used for an off-chain storage mechanism. The homomorphic encryption based on the Krum updates is used for encryption processes. The communication frequency for every round is calculated. Here, 5 local clients are assigned to a global model for training. Table 5 and Figure 4 depict the proposed work of melanoma feature extraction using the CapsNet architecture. Figure 4 is the normalised feature value obtained from the feature extracted value calculated in the table. From the analysis, it is seen that all the types of melanoma detected show asymmetry above 50%, which proves the skin lesion to be malignant.

Table 5. Melanoma feature extraction based on CapsNet model

Melanoma Type	Classified Image	Segmented	Features
SSM	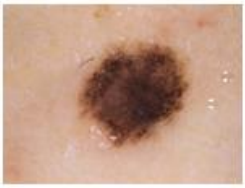		Asymmetry: 1.437 Border Irregularity: 73% Diameter: 387.96 pixels Dotted Vessels: 10% Irregular Streaks: 60%
NM		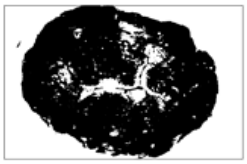	Asymmetry: 1.234 Border Irregularity: 68% Diameter: 708 pixels Dotted Vessels: 75% Irregular Streaks: 40%
ALM	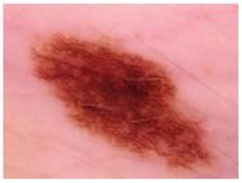	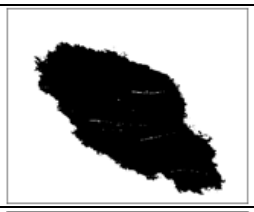	Asymmetry: 1.74 Border Irregularity: 79% Diameter: 708 pixels Dotted Vessels: 39% Irregular Streaks: 48%
LLM		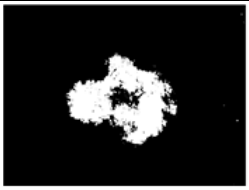	Asymmetry: 1.33 Border Irregularity: 81% Diameter: 154 pixels Dotted Vessels: 51% Irregular Streaks: 37%
DM			Asymmetry: 1.57 Border Irregularity: 65% Diameter: 518 pixels Dotted Vessels: 19% Irregular Streaks: 38%

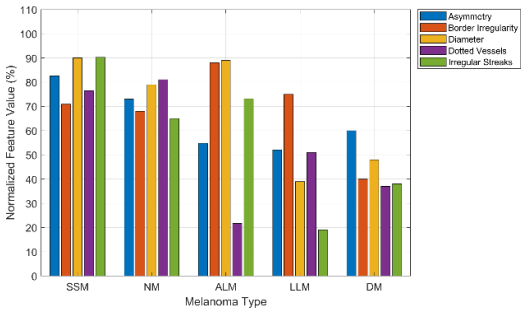

Fig. 4 Melanoma feature vectors using CapsNet

Based on morphological features, melanoma is classified by type. Ensemble transfer learning based classification produces the type detection based on the features it obtained. Asymmetry is high in SSM, and border irregularity is high in NM and ALM. These basic features help in the diagnostic criteria for detecting melanoma. The highest irregular streaks found in the SSM type help in the classification of spreading melanoma. In NM, 80% dotted vessels were found. Thus, each subtype serves as a unique fingerprint for the identification of melanoma. The classification of the most aggressive based on lesion images produced more accurate results.

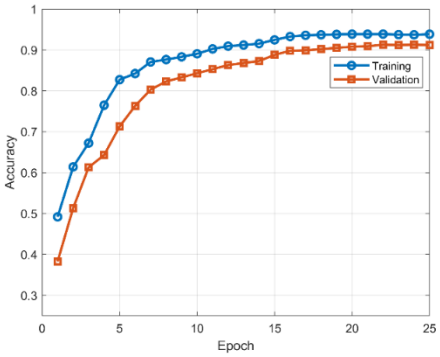

(a) Accuracy plot of training model

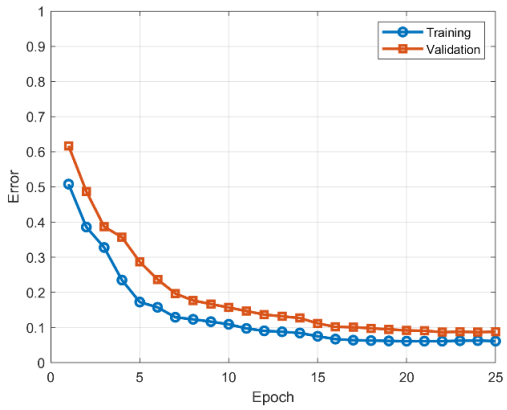

(b) Error plot of training model

Fig. 5 (a) Accuracy, and (b) Loss for the proposed melanoma classification in the local model.

Figure 5(a) and (b) is the accuracy and error percentage plot for proposed melanoma detection and classification using the CapsNet architecture and Ensemble Transfer learning. It is seen that the training accuracy converges at 94%, whereas the validation accuracy converges near 91% in Figure 5(a). This small gap is due to the lower overfitting of the HAM10000 datasets in the proposed model.

The accuracy and error are mere interpretations of the image preprocessing techniques, CapsNet, and Ensemble Transfer learning for classification processes. The proposed model produced a smooth rise without the erratic jumps, which signifies the dataset balances. The error converges at 0.09% for the validation set in Figure 5 (b). From the error and accuracy plot, after epoch 15, both the training and validation start to converge, thus showing the robustness of the CapsNet architecture for learning the core features quickly.

Table 6 is presented to showcase the robustness of the training model using the CapsNet architecture, where the proposed model shows 24.3% improvement over the CNN models on average. The probability of the observance (p) values is calculated, where the proposed models stand <0.005, proving the model to be more reliable.

Table 6. comparison of CNN and proposed capsnet model for the proposed framework using the ABCDE rule of melanoma feature extraction

Feature	CNN-Strength %	Proposed CapsNet Strength %	p-value
Asymmetry	58	83	0.002
Border	64	86	0.001
Color	55	79	0.003
Diameter	62	88	0.001
Evolution	56	81	0.002
Dermoscopic Pattern	60	84	0.001

Table 7. Evaluation parameters for the local nodes in the federated learning framework

Local Models	ACCURACY	PRECISION	RECALL	F1
Node 1	90.5%	91.2%	89.7%	90.44%
Node 2	89.97%	90.65%	90.1%	90.37%
Node 3	89.89%	90.12%	89.9%	90.01%
Node 4	90.7%	91.3%	89.8%	90.5%
Node 5	90.9%	91.85%	90.6%	91.22%

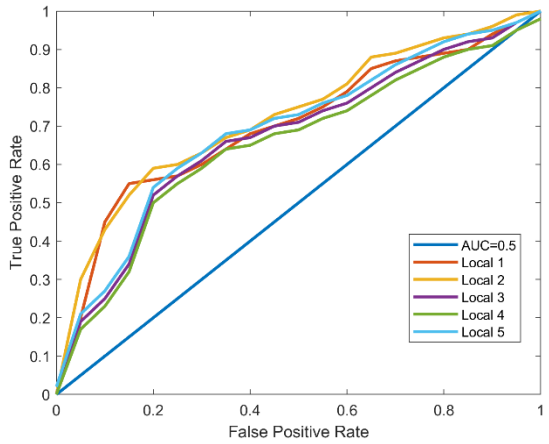

Fig. 6 ROC for the local nodes

In Table 7, the evaluation parameters are tabulated for the local models of the federated learning framework. It is seen that all the model scores have an accuracy and F1 score of approximately 90%, indicating the strong generalisation, feature extraction among local clients, and good data training by the global model. In the federated framework, the local model uses the datasets from the global model in equal proportions. In practical melanoma detection, low false positives and false negatives are crucial, and the proposed model balances them well. Thus, the local models using the proposed image processing techniques provide trustworthy predictions and perform stably, which can be scaled up to multiple hospital scenarios.

In Figure 6, the Region of Curve (ROC) is plotted for 5 local clients connecting to the global model. All the local nodes perform the marginal line, indicative of the discriminative features of the local clients. Every individual node sharing the global datasets equally is contributing meaningfully and maintains the discriminative function with good reliability. This plot helps to identify the function of each local client, connecting the global model using the proposed model.

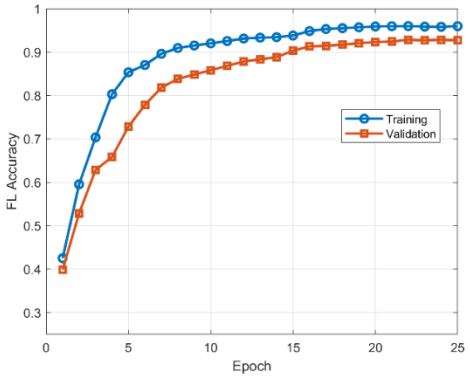

(a)

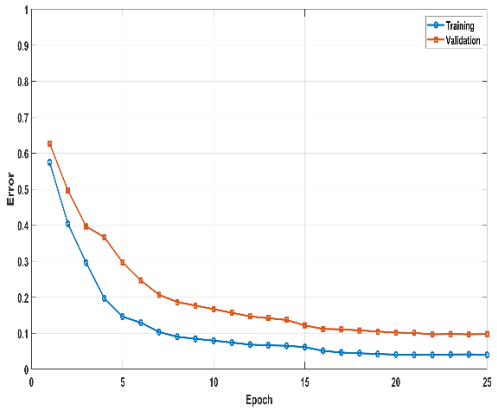

(b)

Fig.7 (a) and (b) Accuracy and loss for blockchain-based federated learning framework.

Figure 7 (a) and (b) contribute to the accuracy and loss value for the Blockchain-based Federated learning framework for the global model and its local clients using the melanoma detection and classification using the CapsNet and Ensemble transfer learning process. Here, the training accuracy converges at 96%, and the validation accuracy converges at approximately 93% in Figure 8(a).

The feature learning, classification, and real-time data updation using the LSTM approach in the global models help achieve high accuracy, starting to converge from 15 epochs. The blockchain network provides fair data contribution and rewards that support the critical melanoma diagnosis tasks. The error calculation approaches 0.07 value for the validation dataset, which is depicted in Figure 8 (b).

Figure 8 represents the test error calculation for the Secured Federated learning framework for melanoma classification using Blockchain Technology. The main objective of using blockchain technology here is to reduce the risk of data poisoning attacks. The hash function based on homomorphic encryption and Krum updates helps detect malicious clients that access the local model.

To test the proposed framework, 30% of the Poisson attacks are framed in the local clients' training model to check the efficacy of the system. It is seen that the BCFL achieves approximately 0.01 error at 100 rounds compared to the conventional FL method, which settles at 0.03%. It is noticed that the BCFL model starts to outperform the conventional FL model at the 20th round itself. The credits of less fluctuation in BCFL are due to the consistent learning in the local model and security upgrades.

Thus, the proposed framework proved to be reliable and stable for the melanoma classification of the patients in a secure manner. Table 8 illustrates the different Blockchain-based FL methods based on their dataset to compare the

efficacy of the proposed framework. Figure 9 provided the poisson attack-based performance of the proposed framework with different percentages of Poisson attack performed using the conventional Federated learning and Blockchain-based FL model, where the proposed work showed higher accuracy comparatively for an increase in the poisson attack.

Table 8. Comparison of accuracy

Ref	Year	Work	Dataset	Accuracy%
[40]	2020	BFCL	FEMINIST	89.03%
[41]	2022	BAFL	MNIST	91%
[42]	2020	BCFL in Medicine	NIH DID	86%
[43]	2025	BCFL for EHR	Imbalanced MNIST Skewed MNIST	91% 93%
[44]	2022	Blockchain for HER	MNIST	89%
[45]	2025	FedViTBloc	HAM10000	67%
[46]	2025	Homographic encryption based FL	HAM10000	91%
[47]	2025	Personalized Multimodal FL	ISIC	92.3%
Proposed Model			HAM10000	93%

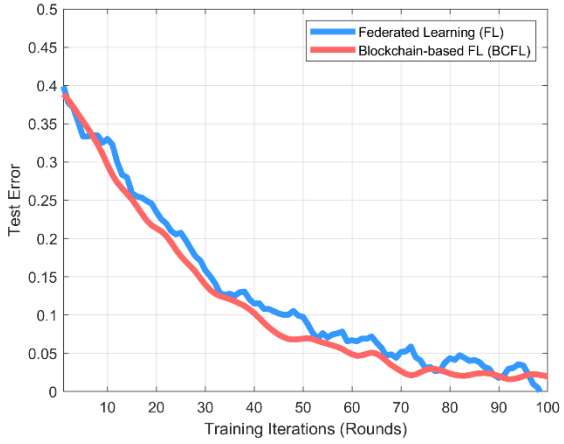

Fig. 8 BCFL vs FL test error calculation for 100 iterations

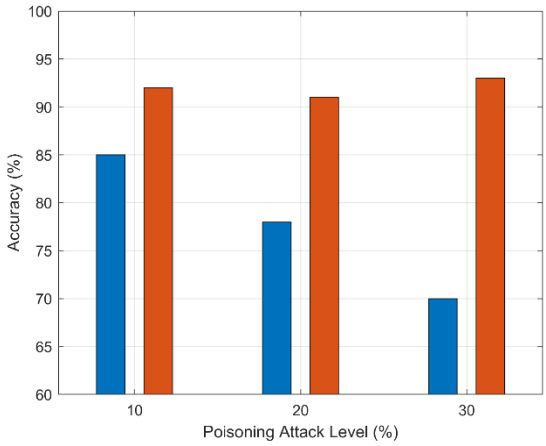

Fig. 9 Poisson attack performance

6. Conclusion

The Secured Federated learning framework for melanoma classification using the CapsNet for feature extraction, Ensemble Transfer learning for classification, and LSTM for weight updation to the global model is accomplished and simulated based on the parameters discussed using the Blockchain technology. The proposed framework and the proposed local client model show an accuracy of 93%. The security of the Federated learning framework is enhanced by the Blockchain technology, where the hash function for every client and krum updates plays the central role. The proposed work is evaluated for normalised feature extraction value for melanoma types, accuracy, and error for the local model, presented evaluation parameters for local models, ROC representation for the local models, accuracy and error calculation for the proposed BCFL framework, and test error for poison attack response of the framework for 100 iterations.

6.1. Future Scope

- The proposed framework can be applied to various disease diagnoses based on the decentralised system.
- The proposed framework applies to the Internet of Medical Things applications.
- It interconnects the image processing techniques with the decentralised systems like Federated learning and Blockchain technologies.

References

[1] International Agency for Research on Cancer, World Health Organisation, Skin Cancer, 2026. [Online]. Available: https://www.iarc.who.int/cancer-type/skin-cancer/

[2] Hensin Tsao et al., "Early Detection of Melanoma: Reviewing the ABCDEs," *Journal of the American Academy of Dermatology*, vol. 72, no. 4, pp. 717-723, 2015. [CrossRef] [Google Scholar] [Publisher Link]

[3] Mirna Šitum et al., "Melanoma-Clinical, Dermatoscopical, and Histopathological Morphological Characteristics," *Acta Dermatovenerologica Croatica*, vol. 22, no. 1, pp. 1-12, 2014. [Google Scholar] [Publisher Link]

[4] Harris Banerjee, "Morphological and Immunophenotypic Variations in Malignant Melanoma," *Histopathology*, vol. 36, no. 5, pp. 387-402, 2000. [CrossRef] [Google Scholar] [Publisher Link]

[5] Jagoda Balaban et al., "Clinical and Morphological Characteristics of Cutaneous Melanoma," *Acta Dermatovenerologica Croatica*, vol. 22, no. 4, pp. 271-277, 2014. [Google Scholar] [Publisher Link]

[6] BS Nikolai Klebanov et al., "Clinical Spectrum of Cutaneous Melanoma Morphology," *Journal of the American Academy of Dermatology*, vol. 80, no. 1, pp. 178-188, 2019. [CrossRef] [Google Scholar] [Publisher Link]

[7] Michael T. Mazur, and Anna-Luise A. Katzenstein, "Metastatic Melanoma: The Spectrum of Ultrastructural Morphology," *Ultrastructural Pathology*, vol. 1, no. 3, pp. 337-356, 1980. [CrossRef] [Google Scholar] [Publisher Link]

[8] Raouf E. Nakhleh et al., "Morphologic Diversity in Malignant Melanomas," *American Journal of Clinical Pathology*, vol. 93, no. 6, pp. 731-740, 1990. [CrossRef] [Google Scholar] [Publisher Link]

[9] Raúl Cabrera, and Francisca Recule, "Unusual Clinical Presentations of Malignant Melanoma: A Review of Clinical and Histologic Features with Special Emphasis on Dermatoscopic Findings," *American Journal of Clinical Dermatology*, vol. 19, no. S1, pp. 15-23, 2018. [CrossRef] [Google Scholar] [Publisher Link]

[10] Amaya Viros et al., "Improving Melanoma Classification by Integrating Genetic and Morphologic Features," *PLoS Medicine*, vol. 5, no. 6, pp. 1-12, 2008. [CrossRef] [Google Scholar] [Publisher Link]

[11] Richard A. Scolyer et al., "Evolving Concepts in Melanoma Classification and their Relevance to Multidisciplinary Melanoma Patient Care," *Molecular Oncology*, vol. 5, no. 2, pp. 124-136, 2011. [CrossRef] [Google Scholar] [Publisher Link]

[12] Ahmad Naeem et al., "Malignant Melanoma Classification using Deep Learning: Datasets, Performance Measurements, Challenges and Opportunities," *IEEE Access*, vol. 8, pp. 110575-110597, 2020. [CrossRef] [Google Scholar] [Publisher Link]

[13] Fengying Xie et al., "Melanoma Classification on Dermoscopy Images using a Neural Network Ensemble Model," *IEEE Transactions on Medical Imaging*, vol. 36, no. 3, pp. 849-858, 2017. [CrossRef] [Google Scholar] [Publisher Link]

[14] Mario Fernando Jojoa Acosta et al., "Melanoma Diagnosis using Deep Learning Techniques on Dermatoscopic Images," *BMC Medical Imaging*, vol. 21, no. 1, pp. 1-11, 2021. [CrossRef] [Google Scholar] [Publisher Link]

[15] Subhayu Ghosh et al., "Melanoma Skin Cancer Detection using Ensemble of Machine Learning Models Considering Deep Feature Embeddings," *Procedia Computer Science*, vol. 235, pp. 3007-3015, 2024. [CrossRef] [Google Scholar] [Publisher Link]

[16] Adekanmi A. Adegun, and Serestina Viriri, "Deep Learning-based System for Automatic Melanoma Detection," *IEEE Access*, vol. 8, pp. 7160-7172, 2020. [CrossRef] [Google Scholar] [Publisher Link]

[17] E. Nasr-Esfahani et al., "Melanoma Detection by Analysis of Clinical Images using Convolutional Neural Network," *2016 38th Annual International Conference of the IEEE Engineering in Medicine and Biology Society (EMBC)*, Orlando, FL, USA, pp. 1373-1376, 2016. [CrossRef] [Google Scholar] [Publisher Link]

[18] Meenalosini Vimal Cruz et al., "Skin Cancer Classification using Convolutional Capsule Network (CapsNet)," *Journal of Scientific & Industrial Research*, vol. 79, no. 11, pp. 994-1001, 2020. [Google Scholar]

[19] Evgin Goceri, "Classification of Skin Cancer using Adjustable and Fully Convolutional Capsule Layers," *Biomedical Signal Processing and Control*, vol. 85, 2023. [CrossRef] [Google Scholar] [Publisher Link]

[20] Zhangli Lan et al., "FixCaps: An Improved Capsules Network for Diagnosis of Skin Cancer," *IEEE Access*, vol. 10, pp. 76261-76267, 2022. [CrossRef] [Google Scholar] [Publisher Link]

[21] Divya, Niharika Anand, and Gaurav Sharma, "Convolutional Neural Network (CNN) and Federated Learning-based Privacy Preserving Approach for Skin Disease Classification," *Journal of Supercomputing*, vol. 80, no. 16, pp. 24559-24577, 2024. [CrossRef] [Google Scholar] [Publisher Link]

[22] Hussain AlSalman et al., "Federated Learning Approach for Breast Cancer Detection based on DCNN," *IEEE Access*, vol. 12, pp. 40114-40138, 2024. [CrossRef] [Google Scholar] [Publisher Link]

[23] Minh Tran et al., *Chapter 3 - CapsNet for Medical Image Segmentation*, Deep Learning for Medical Image Analysis (Second edition), Academic Press, pp. 75-97, 2024. [CrossRef] [Google Scholar] [Publisher Link]

[24] Hong Zhang et al., "Attentive Octave Convolutional Capsule Network for Medical Image Classification," *Applied Sciences*, vol. 12, no. 5, pp. 1-16, 2022. [CrossRef] [Google Scholar] [Publisher Link]

[25] Sulbha Yadav, and Sudhir Dhage, "TE-CapsNet: Time Efficient Capsule Network for Automatic Disease Classification from Medical Images," *Multimedia Tools and Applications*, vol. 83, no. 16, pp. 49389-49418, 2023. [CrossRef] [Google Scholar] [Publisher Link]

[26] Mahmood Ul Haq et al., "Capsule Network with its Limitation, Modification, and Application-A Survey," *Machine Learning and Knowledge Extraction*, vol. 5, no. 3, pp. 891-921, 2023. [CrossRef] [Google Scholar] [Publisher Link]

[27] Youyang Qu et al., "Blockchain-Enabled Federated Learning: A Survey," *ACM Computing Surveys*, vol. 55, no. 4, pp. 1-35, 2022. [CrossRef] [Google Scholar] [Publisher Link]

[28] Muhammad Shayan et al., "Biscotti: A Blockchain System for Private and Secure Federated Learning," *IEEE Transactions on Parallel and Distributed Systems*, vol. 32, no. 7, pp. 1513-1525, 2020. [CrossRef] [Google Scholar] [Publisher Link]

[29] Shafia Riaz et al., "Federated and Transfer Learning Methods for the Classification of Melanoma and Nonmelanoma Skin Cancers: A Prospective Study," *Sensors*, vol. 23, no. 20, pp. 1-27, 2023. [CrossRef] [Google Scholar] [Publisher Link]

[30] Rahil Garnavi, Mohammad Aldeen, and James Bailey, "Computer-Aided Diagnosis of Melanoma using Border-and Wavelet-based Texture Analysis," *IEEE Transactions on Information Technology in Biomedicine*, vol. 16, no. 6, pp. 1239-1252, 2012. [CrossRef] [Google Scholar] [Publisher Link]

[31] A.K. Vikey, and Deepali Vikey, "Primary Malignant Melanoma, of Head and Neck: A Comprehensive Review of Literature," *Oral Oncology*, vol. 48, no. 5, pp. 399-403, 2012. [CrossRef] [Google Scholar] [Publisher Link]

[32] Stephanie L Skala et al., "Comprehensive Histopathological Comparison of Epidermotropic/Dermal Metastatic Melanoma and Primary Nodular Melanoma," *Histopathology*, vol. 72, no. 3, pp. 472-480, 2018. [CrossRef] [Google Scholar] [Publisher Link]

[33] Angela Moreno et al., "Histologic Features Associated with an Invasive Component in Lentigo Maligna Lesions," *JAMA Dermatology*, vol. 155, no. 7, pp. 782-788, 2019. [CrossRef] [Google Scholar] [Publisher Link]

[34] Patricia Basurto-Lozada et al., "Acral Lentiginous Melanoma: Basic Facts, Biological Characteristics and Research Perspectives of an Understudied Disease," *Pigment Cell & Melanoma Research*, vol. 34, no. 1, pp. 59-71, 2020. [CrossRef] [Google Scholar] [Publisher Link]

[35] T.M. Hughes et al., "Desmoplastic Melanoma: A Review of its Pathology and Clinical Behaviour, and of Management Recommendations in Published Guidelines," *Journal of the European Academy of Dermatology and Venereology*, vol. 35, no. 6, pp. 1290-1298, 2021. [CrossRef] [Google Scholar] [Publisher Link]

[36] Brendan McMahan et al., "Communication-Efficient Learning of Deep Networks from Decentralized Data," *Proceedings of the 20th International Conference on Artificial Intelligence and Statistics*, vol. 54, pp. 1273-1282, 2017. [Google Scholar] [Publisher Link]

[37] Geming Xia et al., "Poisoning Attacks in Federated Learning: A Survey," *IEEE Access*, vol. 11, pp. 10708-10722, 2023. [CrossRef] [Google Scholar] [Publisher Link]

[38] Philipp Tschandl, Cliff Rosendahl, and Harald Kittler, "The HAM10000 Dataset, a Large Collection of Multi-Source Dermatoscopic Images of Common Pigmented Skin Lesions," *Scientific Data*, vol. 5, no. 1, pp. 1-9, 2018. [CrossRef] [Google Scholar] [Publisher Link]

[39] K. Scott Mader, Skin Cancer MNIST: HAM10000 A Large Collection of Multi-Source Dermatoscopic Images of Pigmented Lesions, Kaggle, 2018. [Online]. Available: https://www.kaggle.com/datasets/kmader/skin-cancer-mnist-ham10000

[40] Yuzheng Li et al., "A Blockchain-based Decentralized Federated Learning Framework with Committee Consensus," *IEEE Network*, vol. 35, no. 1, pp. 234-241, 2021. [CrossRef] [Google Scholar] [Publisher Link]

[41] Lei Feng et al., "BAFL: A Blockchain-based Asynchronous Federated Learning Framework," *IEEE Transactions on Computers*, vol. 71, no. 5, pp. 1092-1103, 2021. [CrossRef] [Google Scholar] [Publisher Link]

[42] Omar El Rifai et al., "Blockchain-based Federated Learning in Medicine," *International Conference on Artificial Intelligence in Medicine*, pp. 214-224, 2020. [CrossRef] [Google Scholar] [Publisher Link]

[43] S.P. Panimalar, and S. Gunasundari, "A Novel Privacy Protection Technique of Electronic Health Records using Decentralized Federated Learning with Consortium Blockchain," *Procedia Computer Science*, vol. 252, pp. 212-221, 2025. [CrossRef] [Google Scholar] [Publisher Link]

[44] Muneera Alsayegh et al., "Towards Secure Searchable Electronic Health Records using Consortium Blockchain," *Network*, vol. 2, no. 2, pp. 239-256, 2022. [CrossRef] [Google Scholar] [Publisher Link]

[45] Gabriel Chukwunonso Amaizu et al., "FedViTBloc: Secure and Privacy-Enhanced Medical Image Analysis with Federated Vision Transformer and Blockchain," *High-Confidence Computing*, vol. 5, no. 3, pp. 1-12, 2025. [CrossRef] [Google Scholar] [Publisher Link]

[46] Sahar Ebadinezhad, and Noor Amer Ahmed, "Privacy-Preserving Federated Learning for Skin Cancer Detection using Homomorphic Encryption and Advanced Deep Learning Techniques," *IAENG International Journal of Computer Science*, vol. 52, no. 7, pp. 2467-2477, 2025. [Google Scholar] [Publisher Link]

[47] Shuhuan Fan et al., "A Personalized Multimodal Federated Learning Framework for Skin Cancer Diagnosis," *Electronics*, vol. 14, no. 14, pp. 1-33, 2025. [CrossRef] [Google Scholar] [Publisher Link]